IEEE Access
Multidisciplinary | Rapid Review | Open Access Journal

Received 1 April 2025, accepted 20 May 2025, date of publication 29 May 2025, date of current version 6 June 2025.

Digital Object Identifier 10.1109/ACCESS.2025.3574996

RESEARCH ARTICLE

Parasitic Monitoring of Road Constructions: Setting Up and Implementing a New System for Pavement-Tyre Friction

ALESSIA LAZZARO[1], MASSIMO MERENDA[2], (MEMBER, IEEE), AND FILIPPO GIAMMARIA PRATICÒ[1]

[1]Department of Information Engineering, Infrastructure and Sustainable Energy (DIIES), University Mediterranea of Reggio Calabria, 89122 Reggio Calabria, Italy
[2]HWA srl—Spin-off UNIRC, 89126 Reggio Calabria, Italy

Corresponding author: Filippo Giammaria Praticò (filippo.pratico@unirc.it)

This work was supported in part by European Commission under the L'Instrument Financier pour l'Environnement (LIFE) SILENT Project "Sustainable Innovations for Long-life Environmental Noise Technologies" under Grant LIFE22-ENV-IT-LIFE-SILENT/101114310, and in part by the LIFE SNEAK Project "Optimised Surfaces against NoisE And vibrations produced by tramway tracK and road traffic" under Grant LIFE20 ENV/IT/000181.

ABSTRACT Tyre-pavement friction influences transport safety, particularly in autonomous vehicles (AVs), where real-time friction estimation impacts critical decisions (e.g., stopping, changing lanes, and deceleration rate). Despite this, there is a lack of methods to have low cost and continuous monitoring. Consequently, this study proposes a novel system to continuously provide on-board microprocessors with updated estimates of tyre-pavement friction as a function of pavement, tyre, meteorological, and driving conditions. To this end, the following main tasks were carried out: 1) In task 1, the problem was modelled, and high-level equations to satisfy were set up for both AVs and human-driven vehicles (HDVs). 2) In task 2, a framework was set up to solve friction-related issues considering critical scenarios involving unconnected vehicles. 3) In task 3, a solution to continuously estimate tyre-pavement friction for AVs and HDVs was set up, and the consequences for connected and cooperative vehicles were analysed and modelled. 4) In task 4, the following conclusions were derived: A) The system herein set up and implemented has outstanding characteristics in terms of small cost. B) It allows for quasi-continuous monitoring of pavement friction, and both long-term and short-term changes can be detected. C) Both points are crucial due to the limitations of common friction monitoring systems in achieving high sampling frequencies. Future research will focus on increasing the number of sets of braking manoeuvres and on the optimisation of the hardware and software of the system to add to the existing onboard system.

INDEX TERMS Dynamics-based method, microcontroller, OBDII, pavement-tyre friction coefficient, real-time estimation.

I. OBJECTIVES

The objectives of the study were confined to the following:

1) To introduce the research environment, highlighting the critical aspects and challenges related to pavement-tyre friction monitoring and the need for efficient real-time and estimation methods.
2) To design and implement a parasitic method for monitoring pavement-tyre friction.
3) To set up the friction estimation system above (based on in-vehicle measurements).

To this end, it is noted that to interpret vehicle dynamic behaviour data and derive real-time information on pavement friction, data and algorithms need to be complemented with investigatory and threshold limits (cf. [1]). These data and pieces of information are going to be transferred to stakeholders (vehicle-to-everything communication, V2X).

The associate editor coordinating the review of this manuscript and approving it for publication was Md. Moinul Hossain.

The final aim is to benefit drivers and autonomous vehicles (e.g., cautious behaviour and speed reduction) as well as road agencies (decision-making about investigation and interventions (e.g., milling and laydown, overlay, bituminous treatments and pertaining maintenance and rehabilitation operations).

To pursue the objectives above, the following tasks were carried out:

1) Analysis of the state-of-the-art (cf. sections ''Introduction'' and ''State-of-the-art'').
2) Set up of the method (hardware and software) and design of the experiments (cf. ''Methodology'').
3) Implementation of the method (cf. ''Design of Experiments and Result''): a.
   a) Vehicle Status Monitoring - Dataset Acquisition Phase.
   b) Data Processing.
   c) Analysis of results.
4) Derivation of conclusions and future work (cf. ''Conclusions and future work'').

II. INTRODUCTION

A. SAFETY AND FRICTION

Road safety is one of the main missions of state departments of transportation (DOT), and one of the key areas of improvement concerns pavement-tyre friction, a central component in the control of vehicle motion [2]. Friction is the force that allows the vehicle to move forward, and in this context, the term traction refers to the friction between the driving wheel and the road surface. Loss of traction is equivalent to loss of grip on the ground, thereby compromising vehicle control. In fact, in a safe driving context, vehicle safety depends on the module of friction available in relation to the dynamic forces acting on the vehicle: it is desirable to have a high coefficient of friction so that it can be applied when needed. More in detail, static friction is the phenomenon responsible for the traction required for the rubber of the tyre to move, under the effect of the force transmitted by the engine, without slipping on the road surface. For example, sufficient static friction allows the tyres to adhere to the road surface, allowing the vehicle to decelerate safely, thus avoiding skidding or longer braking times. During acceleration, deceleration, or manoeuvring, the wheels transmit larger-than-normal dynamic forces to the pavement, requiring more friction to ensure safe driving. Under normal conditions, the tyre/road contact area is sufficiently stable and friction is provided, but during severe manoeuvres the additional forces may exceed the available friction, causing the tyres to slip [3]. Friction forces for a specific combination of road surface and tyre depend on various factors, such as tyre load and pressure, tread depth and shape, road surface characteristics, presence of water or ice on the pavement, driving speed, and other [3]. These factors affecting Skid resistance/friction can be divided into main groups: vehicle factors, road surface characteristics, road geometry, environmental conditions, and driving factors. Several studies point out how accident rates are affected by the lack of friction on the pavement, but it is difficult to isolate the effect of poor friction on accident risk: drivers adapt their driving behaviour based on many factors, such as the appearance of the road environment, weather conditions, tyre noise, and vehicle skidding movements. Under critical conditions, drivers adapt mainly to the appearance of the environment rather than the actual friction conditions [4].

With the emergence of the coexistence of Human-Driven Vehicles (HDV) and Autonomous Vehicles (AV) in modern and future society, the importance of friction forces between roads and tyres grows significantly, influencing safety and efficiency in today's mixed AV and HDV traffic scenarios. In this context, tyres play a key role, as they are responsible for generating the forces and moments that determine vehicle movement. Given the strong interdependence between the operating conditions of the road surface and the instantaneous forces and moments generated, real-time estimation of the pavement-tyre friction coefficient is set to play a key role in improving the performance of vehicle control systems. This result also contributes to improving the level of pedestrian confidence in automated vehicles [5]. In order to increase the level of confidence, it is necessary to adopt methods that link the operating conditions of the road surface and the vehicle [6]. For example, there is a growing idea of turning tyres into active components, which, until now, have been considered passive elements in most vehicle control systems, in the sense that they do not provide real-time information [7], [8].

Unfortunately, friction forces cannot be measured directly, but only observed or estimated. Most observation and estimation techniques require exciting the longitudinal dynamics of the vehicle, which conflicts with the initial objective of stabilising the vehicle. In addition, the dynamic nature of friction and its dependence on boundary variables make it essential to design a real-time solution capable of correctly estimating the mu/speed curve, ensuring a higher level of safety. This integrated solution would allow the system to control the estimation of the traction force more effectively and accurately. The motivation for this research is to prevent the failure of existing control systems due to inadequate model assumptions, taking into account the interdependence between the operating conditions of the road surface and the instantaneous forces and moments generated. Currently, many cars are not equipped with real-time active safety control systems, necessitating the implementation of low-cost solutions that improve existing control structures for pavement-tyre forces. This approach will enable the development of innovative solutions that enhance road safety in mixed traffic scenarios, improving vehicle driving and user confidence in new automated driving systems.

B. ACCEPTANCE, INVESTIGATORY, AND THRESHOLD LEVELS

Another problem is that, as is well known, friction requirements vary over time (from construction to operations) and

over space (because of the differences in road type). Indeed, the requirements after the construction (or maintenance) refer to acceptance procedures. Unfortunately, after the construction, during operations, friction undergoes daily, seasonal, and long-term variations, resulting in an initial and minor increase and after an important decay. During the decay process it is essential to detect the Investigatory Level (IL), that is to say, the level of skid resistance at or below which a site investigation is to be undertaken, and the Threshold Level (TL), which is the trigger level for determining priority for treatment. While acceptance procedures are one-shot measurements (usually between the 15th and the 180-th day after the construction), operation-related levels (IL, TL) refer to a long period (e.g., 10 years), where apart from the decay due to the traffic and environmental actions further instantaneous causes could drastically change the friction (oil and diesel spillages and contamination and loose gravel, [9]). Under these hypotheses, it is of paramount importance to increase the sampling frequency of friction data gathering. This need has become even more important for motorcyclists and autonomous vehicles. Unfortunately, the increase in sampling frequency through traditional testing machines is limited by practical and economic reasons and this makes it important to set up and implement new systems to continuously gather friction data for management, safety, economic, and sustainability purposes.

C. MODELS AND THEORIES FOR FRICTION PREDICTION

One of the key parameters for implementing a safe driving support system is the tyre/pavement interaction force since the forces generated by the tyres are the primary forces affecting planar vehicle motions because they are the only force sources that a vehicle has from the ground [10]. Many surveys on vehicle traffic safety have shown that the tyre road friction coefficient (TRFC) is correlated with the probability of an accident. Therefore, accurate TRFC information is essential to improve the performance of active safety systems. For example, active safety systems such as antilock braking systems (ABS), among other functions, have the task of maintaining the traction between the tyres and the road at an optimal value [11]. Hence, an estimate of the friction parameter in real-time, while vehicle motion, and using easy access measurements (acceleration, speed, steering angle, etc.), can provide the driver (or the autopilot system) a timely warning of a possible loss of friction, which results in avoiding an imminent exit route [12], thus helping to avoid road accidents. From theory, it is known that the magnitude, in particular the maximum value, of the traction is represented by the friction circle. As shown in Figure 1, the graph represents the theoretical limit of grip (friction) of a tyre in both lateral and longitudinal directions, i.e., in the turning, acceleration and braking scenarios. From the graph above, it can be seen that tyre friction forces are physically limited by the road surface coefficient of friction (μ) and the instantaneous normal tyre forces. Specifically,

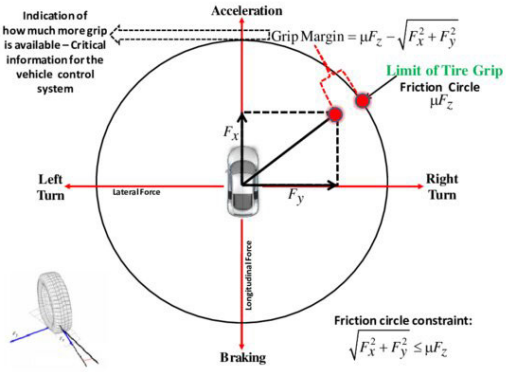

FIGURE 1. Tyre friction circle [15].

under normal driving conditions, the friction force is not fully utilised, and the forces developed by the tyre lie within the friction circle. When inputs are imposed on a tyre, a relative movement occurs between the tyre structure and the road surface, referred to as tyre slip [13]. More precisely, the slip percentage or slip is defined as follows [14]:

$$S = \frac{\omega_w r_w - v_w}{v_w} \tag{1}$$

where r_w is the wheel radius, ω_w is the driven wheel's circumferential velocity, and its absolute velocity v_w.

When the limit of the friction forces is exceeded, there is a serious risk of losing control of the vehicle, i.e. the vehicle's ability to respond adequately to the driver's commands is lost. This concept applies to any type of vehicle, both HDV and AV. In fact, any vehicle's active safety systems stabilise the vehicle by controlling tyre forces. However, they work well only when the commanded tyre forces are within the friction limit [16]. It is, therefore, fundamental to monitor and manage the level of grip between the tyre and the road to understand the maximum value available in order to design a control system that acts to guarantee safe driving over a wider range of conditions, that is, a system that is able to increase vehicle stability and manage the dynamic behaviour of the tyre. These motivations drive the search for a 'road-adaptive' algorithm that gives input on the state of the vehicle and its environment and returns information on the coefficient of friction tyre/pavement.

There are various approaches for estimating the pavement-tyre friction coefficient. An initial subdivision made by [11] divides them into three main categories: off-board sensors, vehicle **dynamics-based approaches**, and **data-driven prediction methods**. Approaches based on off-board sensors require fewer measurement variables and are less sensitive to the dynamic response of the vehicle but require the installation of additional sensors on production vehicles. Vehicle dynamics-based approaches, on the other hand, utilise onboard sensors, offering a cost-effective and efficient estimation of the friction coefficient in real-time. Alternatively, a neural network can be used to describe the behaviour of tyres but, this data-driven approach requires a complete

dataset in order to achieve a prediction accuracy that is high and applicable in every scenario.

Considering the advantages of each strategy, the main objective of this research work is to put together a friction estimator based on in-vehicle measurements and the observation of the dynamic behaviour of vehicles.

Within this approach, research techniques are divided into two categories: **cause-based** and **effect-based** methods [17].

- **Cause-based methods** involve an estimation on the basis of the parameters that cause the change in the value of the friction coefficient. For example, causes can be classified into vehicle parameters, tyre parameters, road lubricant parameters, and road parameters [18]. Then, having measured, directly or indirectly, the most significant causes, a friction model is used to obtain the estimate.
- **Effect-based method**, on the other hand, involves measurements of the effects of a change in the value of friction. In the latter method, there is a further subdivision, such as methods based on optical sensors, acoustic sensors, and tyre aligning moment.

This subdivision includes the slip-based approach used in this work because it does not require the use of complex instrumentation for data collection, unlike the other approaches. This choice is also justified in tyre-turning, where one tends to use the same approach to derive parameters from the standard sensors available in the car, which depend directly or indirectly on friction, and then find rules to estimate the maximum friction forces that can be used for braking or cornering [14]. Slip-based estimation methods are defined as a technique for estimating the tyre-pavement friction coefficient [18].

Figure 2 shows the existence of direct proportionality between the friction coefficient and slip for low slip ratios before saturation. This direct relationship is present for each curve, each defined for a particular surface. The value of the slope, called the slip slope, contains sufficient information to provide an accurate value of friction [14]. In addition to defining the approach to be followed on how to collect the data needed to estimate the friction coefficient, it is necessary to define how to process the data collected for the prediction of the latent variable. Below are mathematical models that can be applied to estimate the coefficient of friction.

D. MODELS FOR FRICTION PREDICTION

Friction is a fundamental phenomenon in many control systems, especially in the field of motion control, and is extremely important in various engineering applications, including automotive safety systems. Accurate modelling of friction has the potential to ensure optimal performance, that is, to improve the quality of safety systems. One of the main challenges in modelling friction is its highly nonlinear nature that can induce unpredictable system behaviour. Therefore, to develop more robust control strategies, the use of robust friction models offers an opportunity to reduce the negative

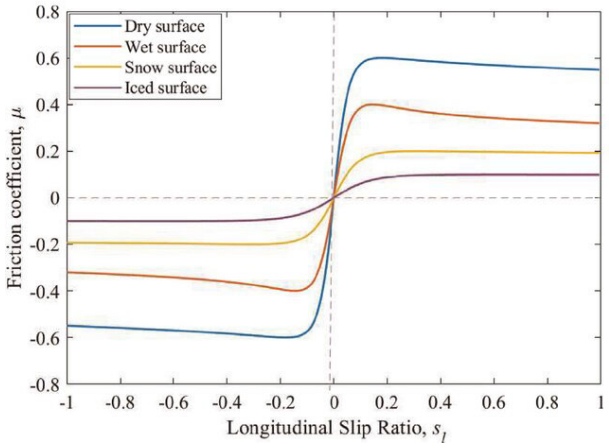

FIGURE 2. Friction coefficient as a function of longitudinal slip ratio [19].

effects of friction on system dynamics. Several friction models have been proposed in the scientific literature to capture the complexity of friction phenomena. These models are mainly divided into categories based on their nature: static models, dynamic models, or hybrid models. Each captures different aspects of friction behaviour [20], [21], [22], [23].

Static friction models, unlike dynamic models, offer a simplified representation and consequently fail to capture the temporal variation of friction under different operating conditions. In fact, static models assume that the friction force depends on the current state of the system without considering time-dependent behaviour, particularly under varying conditions of temperature, humidity, and road surface roughness. These assumptions make these models suitable for systems in which friction does not exhibit complex transient behaviour, but only fixed relationships between variables. The most common static model is the Coulomb friction model, which represents friction as a constant force acting during the displacement of an object subjected to a longitudinal force while the block is pressed into a plane with a normal force. The estimated force is proportional to the normal load and independent of velocity. Consequently, not in all real conditions is the coefficient of friction represented by Columb's model; rather, these coefficients represent a certain value for a particular running condition. Another widely used static model is the viscous friction model, in which friction depends linearly on velocity. The result is a linear approximation of friction, and the validity of the model depends on the operating conditions of the system. While static models fail to represent either the transition between static and dynamic friction or the temporal behaviour of friction during acceleration and deceleration, dynamic or hybrid models, on the other hand, are more sophisticated models and are needed to provide real-time estimates of available friction. The dynamic nature of this model allows it to continuously adapt to changes in driving conditions and thus to represent phenomena that change over time, such as vehicle behaviour, changes in speed and temperature, road

conditions, or tyre deterioration. Dynamic friction models are better suited to capture transient phenomena and are typically described by differential equations, making them more computationally intensive but necessary for high-precision control and for systems with rapid or frequent changes in motion. One of the most widely used dynamic models is Dahl's model. This model accounts for friction as a function of displacement, introducing a hysteresis effect that models the gradual increase in friction forces until sliding. An extension of Dahl's model, LuGre's model, incorporates velocity-dependent behaviour and captures phenomena such as the Stribeck effect, in which friction decreases as velocity increases after overcoming static friction.

The choice of friction model depends largely on the specific requirements of the application. For automotive safety systems, modelling is an essential object of study to provide accurate estimates. Although advanced dynamic models can offer higher accuracy, they often involve significant computational demands, making them less suitable for real-time applications. Therefore, it is necessary to introduce an approach that balances the accuracy of friction estimation with the computational efficiency of the model.

In this study, we propose a dynamic model to estimate the pavement-tyre friction coefficient in real-time. The proposed model captures the temporal evolution of the system, despite its simplified structure, and is suitable for real-time implementations due to its computational efficiency. This model has achieved an optimal balance between computational efficiency and predictive accuracy. This makes our approach ideal for integration into intelligent vehicle safety systems, where timely and accurate friction estimation are key parameters for adapting control strategies to road conditions. Indeed, the ability to estimate friction in real-time makes the proposed model particularly advantageous for dynamic driving conditions, such as changes in the road surface or weather conditions, where rapid adjustments are critical to maintaining vehicle stability and performance.

If the approach was successful, this (data-driven) model herein introduced would be fruitful. Indeed, it would allow accurate estimation of the tyre-pavement friction coefficient using a direct method and using sensors that could be integrated into the on-board system, thus avoiding the use of external sensors.

In addition, such a set-up would provide a real-time model, with advantages in the management of critical conditions, in the reduction of accidents and benefits deriving from not using space-intensive and static solutions.

III. STATE-OF-THE-ART

Understanding road friction in real-time is key to improving vehicle safety, especially under challenging environmental conditions. This section reviews major advances in tyre-pavement friction estimation, focusing on methods of integration between vehicle dynamics model and on-board sensors, i.e., vehicle dynamics-based approaches.

The paper [24] aims at real-time friction coefficient prediction aimed at enhancing the performance of vehicle dynamics control systems like ABS, traction control systems (TCS), and electronic stability control (ESC). Using a multi-sensor signal fusion approach, the method adapts to different vehicle dynamics and control modes. It predicts friction during steering without braking, uses simplified models for active braking scenarios, and employs a neural network for high-intensity braking. Ground tests confirm the method's accuracy and promptness in predicting friction, ensuring effective and timely vehicle control.

In a similar way, the article [25] develops a pavement-tyre friction coefficient estimation algorithm based on vehicle lateral dynamics. The method uses a tyre lateral force model, parameterized by factors such as slip angle, normal force, and cornering stiffness. A real-time parameter identification algorithm, based on differential GPS and gyroscope measurements, is utilized to estimate the pavement-tyre friction coefficient. The experiments, conducted on dry and slippery road surfaces, show the effect of the slip angle amplitude on estimation accuracy. Experimental results highlight the impact of slip angle amplitude on estimation accuracy, with smaller slip angles leading to reduced precision.

Building on test-based experimental methods, the authors [26] designed an estimation approach that fuses dynamic and visual data to determine the maximum tyre-pavement grip coefficient. Using an intelligent electric vehicle as test platform, the method integrates real-time measurements of vehicle dynamics with visual road condition data captured via an onboard camera. The study specifically distinguishes two conditions on the basis of colour: wet asphalt is dark grey and has a higher clarity of texture than dry asphalt.

Further contributing to this field, [27] proposes a method for friction estimation within a steering system controlled by a dedicated module. This method calculates total friction by estimating steering load gain and hysteresis, using these parameters alongside a reference model. The integration of steering dynamics with friction estimation provides a more comprehensive understanding of the vehicle's interaction with the road.

A different approach is presented in [28], which introduces a system for monitoring the coefficient of friction by measuring tread force via sensors embedded anchored between the tyre structure and the tread. This method allows for the detection of small discrete tread element slips in contact with the roadway, enabling real-time monitoring of friction estimation before the entire tyre footprint experiences slip.

In Ahn's paper, [29], a robust prediction method integrating lateral and longitudinal dynamics is presented. This integrated estimator expands the operational range of friction estimators by utilizing a nonlinear observer based on vehicle lateral dynamics and a recursive least squares method

for longitudinal slip and traction force estimation. The system, equipped with standard ESC sensors, demonstrates effectiveness across varying road surfaces and steering excitations, making it adaptable to sudden changes in surface conditions.

This problem calls for high-level management across interdisciplinary research fields (cf. [30]), including 1) Continuous monitoring of friction (currently the friction is monitored only once per year on highways). 2) Material science (where efforts are devoted to improving the mechanical and chemical resistance of pavements against sudden decreases). 3) Automotive-related and electronic-related efforts, where autonomous vehicles need to continuously update deceleration curves based on friction available.

The study in [16] introduces three algorithms for tyre-pavement friction coefficient estimation, tailored to the availability of different sensors. These methods utilize a combination of GPS, engine torque, brake torque, and accelerometer data, depending on the vehicle's sensor configuration. Each algorithm estimates the longitudinal force on the tyre, the longitudinal slip ratio on the wheel, and the friction coefficient, with experimental results validating the reliability of these methods across various scenarios.

Lastly, the studies [10] and [17] focus on applications in specific vehicle types, such as snowplows. In [17], an autonomous wheel-road friction maintenance system is developed for snowplows, utilizing a lateral force measurement approach to assess road surface conditions and control de-icing applications. The system is designed to operate under noisy conditions caused by road surface irregularities, with a filtering technique introduced to improve measurement accuracy.

Similarly, [10] presents a real-time friction coefficient measurement system for winter maintenance vehicles. This system, relying on differential GPS and a non-linear longitudinal tyre force model, is capable of distinguishing between different levels of road surface friction and rapidly detecting abrupt changes, ensuring enhanced operational safety for snowplows.

Alternative method for estimating the tyre-pavement friction coefficient is introduced by paper [31], whose goal is to increase the safety of autonomous vehicles i.e., to decrease the recklessness in driving decisions and optimize navigation. The work exploits in-vehicle sensory fusion and Reinforcement Learning techniques. In addition, where possible, it integrates data from co-infrastructure via Vehicle-to-Infrastructure (V2I) communication. Experimental results show that the approach introduced by the work provides excellent robustness by improving the prediction of the system to surface variations and different driving dynamics.

In summary, the current state-of-the-art demonstrates advancements in real-time pavement-tyre friction estimation by exploiting different approaches. These advancements offer a solid foundation for continued innovation, particularly in the pursuit of more accurate friction estimation systems that can improve vehicle safety and performance under different driving conditions.

IV. METHODOLOGY

In this work, an innovative solution has been proposed for tyre-pavement friction monitoring in real-time through the interaction of different on-board components (cf. Figures 3 and 4).

At the core of this system, there is the **STM32L475** board, which serves as the central data collection hub and performs the real-time estimation of the friction coefficient. The board is equipped with the **LSM6DSL** module, a sensor unit that captures acceleration and angular velocity values at a fixed sampling frequency. The accelerometer sensor measures acceleration forces along three axes, providing data on the vehicle's dynamics, while the gyroscope measures angular velocity around the same axes, capturing information on the vehicle's angular movements.

Supporting the STM32L475 board, the **iLC Diagnostic** (OBDII/EOBD Scan Tool, where OBD is an abbreviation of On-Board Diagnostics, 'E' indicates European and 'II' indicates the second generation of the integrated diagnostic system) serves as the vehicle interface. It communicates with the vehicle's CAN Bus (Controller Area Network, cf. Figure 3, left), which is a vehicle communication network that allows different electronic control units (ECUs, cf. Figure 4)) within the vehicle to exchange information. Although CAN is still the only method to get ''full access'' to your car data, OBDII only provides access to a limited subset of data. However, the OBDII can actively query the ECUs for specific information or passively monitor all messages transmitted on the bus. The data extracted from the vehicle are then transmitted to the M5Stamp-C3 Mate (ESP32-C3, cf. Figure 4), a microcontroller belonging to the M5Stack family featuring an integrated Wi-Fi antenna. The **M5Stamp-C3** acts as an intermediary between the PC and the iLC Diagnostic tool, enabling the acquisition of vehicle information at regular intervals, which is then processed by the STM32L475 board to produce real-time friction estimates. The entire system is shown in Figure 4, which illustrates how the information collected from the STM32 board is extracted through the chain of devices and processes used in this study. In more detail, vehicle speed data, obtained directly from the engine ECU system, is extracted through the OBD port. Connected to this port is the iLC Diagnostic device, which is connected via Wi-Fi to the M5 Stamp-C3 Mate device. The latter is connected to the STM32L475 board via UART interface, where the LSM6DSL module is integrated.

In the proposed system architecture, the iLC OBDII device establishes a dedicated wireless access point (''WiFi_ODBII'') without authentication, allowing seamless and immediate connection by the ESP32-C3 module. This plug-and-play configuration ensures rapid deployment in real-world conditions without requiring user intervention, pairing procedures, or additional software setup.

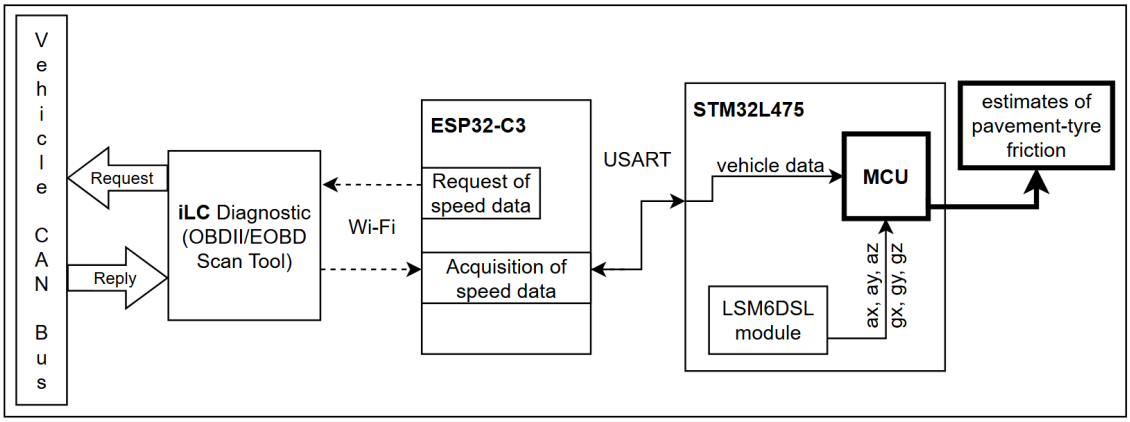

FIGURE 3. Hardware set up.

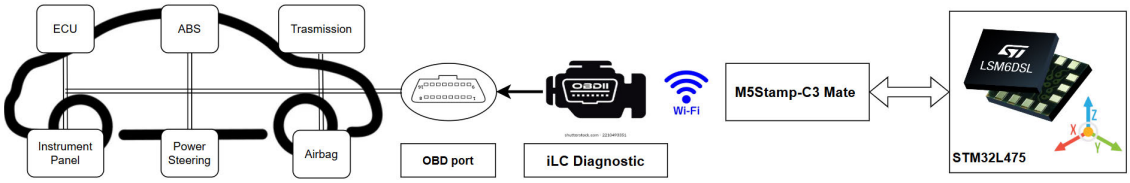

FIGURE 4. System and vehicle.

Alternative wireless protocols, such as ZigBee [32], were considered but discarded due to intrinsic limitations. ZigBee, while energy-efficient and suitable for low-data-rate sensor networks, offers a maximum throughput of 250 kbps under IEEE 802.15.4, significantly lower than Wi-Fi standards supported by ESP32 modules (up to several Mbps). More importantly, ZigBee is not natively compatible with most commercial OBDII interfaces, and its adoption would necessitate non-trivial hardware modifications and software abstraction layers to ensure data interoperability.

Given the moderate volume of diagnostic data, the use of a Wi-Fi-based link ensures sufficient bandwidth and full compatibility with components, thus enabling robust real-time communication within the system. For these reasons, the "WiFi_ODBII" solution was selected as the most efficient and scalable option for friction monitoring in vehicular environments.

A. ILC DIAGNOSTIC SETUP

Modern cars are equipped with the On-board Diagnostic (OBDII) System [33], which is a standard that requires a connection interface, called the OBDII port, for diagnostic test equipment.

The connection of the OBDII reader to the vehicle CAN bus via the 16-pin OBDII connector near the steering wheel allows access to diagnostic information generated by the ECU to monitor the status of the car. The standard OBDII defines several communication protocols for data transfer on the interface, which include: *ISO 9141-2*; *ISO 14230-4* (also known as KWP2000); *ISO 15765* (also known as CAN), the most common protocol; *SAE J1850 VPW* (Variable Pulse Width); *SAE J1850 PWM* (Pulse Width Modulation).

TABLE 1. AT commands used and their description.

AT Command	Description
ATE0	Echo off
ATSP0	Set protocol to auto
ATH0	Headers Off
0100	Search for set protocol
010D	Vehicle speed in kilometers per hour

The transferred data requires a conversion from OBDII language to text format data. This study is carried out by the *EU iLC OBDII* device, which is connected to a vehicle's OBDII port. It reads and interprets messages according to one of the five OBDII protocols, thus defining a link between the vehicle and another device, such as a PC.

The converter *iLC* used in this work transmits diagnostic data via Wi-Fi to the *ESP32-C3* board. Having noted the IP address, 192.168.0.10, and the port of the *ODBII*, 35000, a connection is established between the two devices: the ESP32-C3 device searches for the Wi-Fi network of the iLC device, named "WiFi_ODBII" and without a password, and once the connection is established, the exchange of message packages can begin. For communication with the iLC, a series of AT commands (where AT stands for Attention) were used both to customise communication settings and to require

information. Table 1 shows the list of commands used in this study.

The AT (or "ATtention") commands sent from the ESP32-C3 device to the iLC device are described below.

- "ATE0" deactivates command echo so that the input command is not repeated in the reply message.
- "ATSP0" configures the interface to select the appropriate communication protocol for the vehicle automatically.
- "ATH0" deactivates the header in response messages, making it easier to read the information.
- "0100" instructs the interface to identify and use the correct protocol for communication with the engine control unit.

The AT command sent to request the speed parameter is "010D".

- "01" →regardless of the protocol used, the OBDII can be used in different modes. There are nine available modes and the first byte indicates that the first mode has been selected. The *Mode 1* corresponds to reading current real-time values from the sensors.
- "0D" →OBDII returns the real-time value of engine speed. Each sensor has a command code called Parameter Identifier (PID), which uniquely identifies the parameter. In the case of speed, the parameter code is '0D' and is indicated in the second byte of the AT command.

The vehicle ECU recognises the code and returns the required information in hexadecimal format within a message.

After the settings defined earlier, the structure of the response message is '41 0D FF'.

- "41" →the first byte is the MODE byte, i.e., it indicates the mode of operation. The "41" is a response from a *Mode 1* request ($01 + 0 \times 40 = 41$);
- "0D" →PID number requested;
- "0xFF" →is the speed value expressed in hexadecimal, which therefore requires conversion to a decimal value. The unit of measurement is Km/h.

Each response ends with the character '>', which is used by the ESP32-C3 board as a reference character to finish reading the response packet.

The frequency at which the command is transmitted is set by knowing that:

- we measured the round trip time by pinging the IP and noticed that the iLC device needs between 1 and 1.5 milliseconds to transmit the data via Wi-Fi, after the request has arrived.
- the status parameters are updated by the vehicle with an update rate that is fixed and vehicle-dependent, the maximum value being 20Hz [34].

This allows a request to be sent with a frequency of up to 100Hz, reading either the updated value or the stored value, but for the purpose of the work the same result is obtained by decreasing the frequency. In particular, we choose to set the value at 1Hz, thus one request per second.

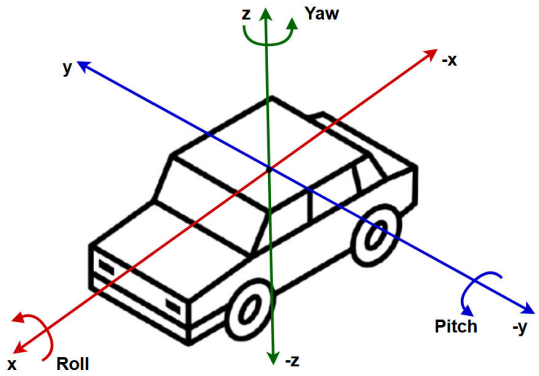

FIGURE 5. Orientation of the accelerometer and gyroscope axes relative to the vehicle.

B. LSM6DSL SETUP

The LSM6DSL module (cf. Figure 4) was used on the STM32L475 board. It is a 3D digital accelerometer and 3D digital gyroscope. Based on the datasheet of the STM32 microcontroller, the reference system adopted is shown in Figure 5. The accelerometer integrated on the board measures longitudinal acceleration, along the x-axis, associated with the direction parallel to the vehicle's motion; lateral acceleration, along the y-axis, is related to transverse displacements with respect to the direction of travel; and finally, acceleration along the z-axis is related to the vehicle's vertical oscillations, mainly induced by irregularities in the road surface. The gyroscope, integrated into the system, provides angular velocity data on the three reference axes. As highlighted in Figure 7, rotation about the x axis is associated with vehicle pitching, while rotation about the y axis represents rolling. Finally, rotation about the z axis corresponds to the yaw of the vehicle.

The following configurations were defined for the accelerometer.

- The *LSM6DSL_ACC_SetFullScale* function is used to set the full-scale range of the accelerometer, which determines the maximum measurable acceleration value. The full-scale range options are typically $\pm 2g$, $\pm 4g$, $\pm 8g$, and $\pm 16g$, where 'g' refers to the acceleration due to gravity ($9.81\ m/s^2$).
- The sampling frequency is set at 104Hz, and the full-scale range is $\pm 4g$. The returned values are in the range *[-4000mg; +4000mg]*.

The following configurations were defined for the gyroscope.

- The *LSM6DSL_GYRO_SetFullScale* function is used to set the full-scale range of the gyroscope, which determines the maximum measurable gyroscope value. The full-scale range options are typically $\pm 125\ dps$, $\pm 250\ dps$, $\pm 500\ dps$, $\pm 1000\ dps$ and $\pm 2000\ dps$, where 'dps' refers to degrees per second.

- The sampling frequency is set at 104Hz, and the full-scale range is ±500 dps. Returned values are in the range *[-500dps; +500dps]*.

C. SENSOR-MCU INTERFACE

The proposed system integrates two primary data sources: the LSM6DSL inertial measurement unit and the OBDII vehicle interface. The LSM6DSL sensor, embedded on the STM32L475 board, communicates via Inter-Integrated Circuit (I^2C) and provides raw accelerometer and gyroscope data sampled at 104 Hz. The OBDII speed data is acquired from the vehicle through a commercial iLC interface, which creates a Wi-Fi access point (“WiFi_ODBII”) and streams diagnostic data to the ESP32-C3 microcontroller.

The ESP32-C3 receives the data using Attention Commands (AT) and relays the extracted vehicle speed information to the STM32L475 via a UART interface. An interrupt-driven mechanism on the STM32 is used to detect new incoming speed data, ensuring synchronisation with Inertial Measurement Unit (IMU) readings and enabling consistent real-time fusion. All computations, including signal integration and friction coefficient estimation, are performed directly on the STM32 board, without reliance on external memory or cloud services. This architecture ensures low-latency processing and complete autonomy of the onboard estimation algorithm.

D. THE ALGORITHM

The algorithm proposed here follows the following steps:

1) HARDWARE SETUP

The defined structure was installed on a Fiat Grande Punto vehicle, as shown in Figure 6. the figure shows the hardware setup installed in the vehicle: on the right, the iLC device; on the left, the STM32L475 board, connected to both the ESP32-C3 and the PC. in detail, the setup is described as follows:

- The iLC device is connected to the OBDII port located under the driver’s side dashboard.
- The ESP32-C3 microcontroller establishes a connection to the iLC device via a Wi-Fi link.
- Once the wireless connection is established, the ESP32-C3 sends AT commands to the iLC converter for customise communication settings. The ESP32-C3 microcontroller was selected because it is a low-cost option with Wi-Fi connectivity, suitable for real-time monitoring of the vehicle’s status.
- At a frequency not exceeding 20 Hz, as indicated in the OBDII datasheet, the ESP32-C3 periodically sends an AT command with the requested PID to the vehicle and waits for the response message.
- iLC device acquires diagnostic data from the vehicle and sends it in a response message to the ESP32-C3 microcontroller.
- The ESP32-C3 reads the message and forwards only the information part to the main board, STM32. The STM32L475 microcontroller was selected for its high performance and integration of accelerometer and gyroscope sensors.
- The STM32L475 board interfaces with the ESP32-C3 board through a Universal Asynchronous Receiver-Transmitter (USART) connection. For each speed data reading, an interrupt is generated on the STM32L475 board to facilitate data transfer, ensuring real-time data acquisition and accurate processing without loss of information.
- This board serves as a data collection center, where post-processing and friction coefficient estimation are performed. The board was securely attached near the vehicle’s center of gravity for better evaluation of longitudinal acceleration (m/s^2).

2) VEHICLE STATUS MONITORING-DATASET ACQUISITION PHASE

The obtained dataset has a structure of eight columns, according to the following order:

- Time: The time instances during which the data were recorded, expressed in hours, minutes, and seconds.
- Acceleration Vector Components: The longitudinal, transverse, and azimuthal components of the acceleration vector.
- Gyroscope Vector Components: The longitudinal, transverse, and azimuthal components of the gyroscope vector.
- Vehicle Speed: The sampling frequency of the vehicle’s speed is significantly lower than that of the acceleration and gyroscope vectors. Consequently, only a subset of rows includes a final column indicating the vehicle’s speed.

3) DATA PROCESSING

Data processing takes place directly at the edge, i.e. on board the integrated microcontroller system, allowing real-time assessment of driving conditions and surroundings. The integration of sensors such as the accelerometer, gyroscope and OBD interface provides a complete view of vehicle and pavement dynamics. This configuration allows the tyre-friction coefficient to be accurately calculated, which is subsequently communicated to the autonomous vehicle’s data processing system for enhanced decision-making and control. Real-time estimation eliminates the need for an SD card (where SD stands for Secure Digital) for data storage, as the coefficient is computed for each data point, negating the necessity to retain the dataset in memory. Furthermore, this setup does not require access to Cloud services. In fact, the selected STM32 microcontroller possesses adequate computational power and memory to post-process the collected data and estimate the friction coefficient in real-time.

For data processing, it is noted that in these experiments:

- The data gathered refer to longitudinal acceleration, speed, and time.

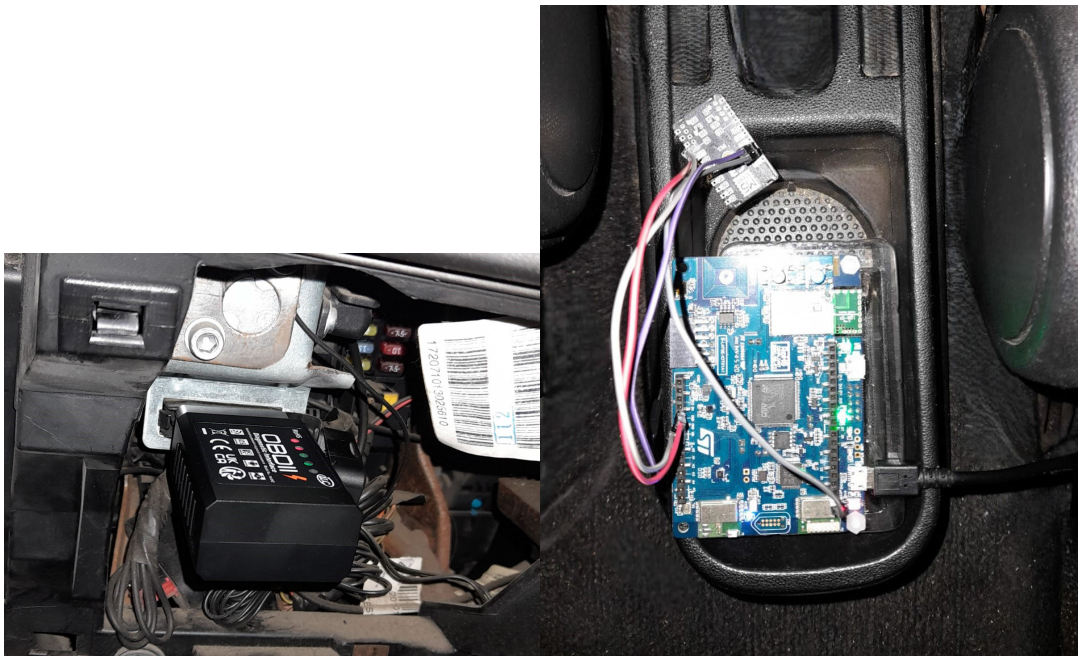

FIGURE 6. The hardware setup installed in the vehicle.

- The algorithms used are as follows:
  1) From the accelerations, the speeds were derived through integration, having at least one known value of speed.
  2) From the speeds the distances were derived through integration.
  3) For each speed change and distance change, the corresponding friction coefficient was derived. It seems noteworthy to point out that aerodynamic resistance was taken into account.

The coefficient of friction $f(V)$ is estimated using the following relation

$$f(V) = \left(V \frac{dV}{dL} - \frac{Ra(V)}{m} \right) \frac{1}{a_g}$$

where: the term $V \frac{dV}{dL}$ represents the kinetic energy per unit distance L covered; $\frac{Ra(V)}{m}$, the aerodynamic resistance, is a velocity-dependent force that increases with the square of the velocity.

E. PRELIMINARY EVALUATION OF PROS AND CONTRAS

When analysing the cost of the device herein set up and vs. the devices currently used, it is important to highlight that the device herein set up has different costs (lower), uses (road users, autonomous, vehicles), precision and dependency on boundary conditions. Therefore, the comparison is affected by these preliminary observations. The system itself herein set up and implemented is cheap. Indeed, its cost can be quantified in no more then 100€.

Furthermore, the overall cost of monitoring does not include any costs related to operations.

In contrast, when considering the traditional systems (e.g., SCRIM and PTP devices, corresponding to the standards CEN/TS 15901-6:2009 and EN13036-4, respectively), the overall cost of monitoring includes both the cost of the device and the cost of manpower.

In summary, the system herein set up and implemented is cheaper than the other traditional methods due to the lower cost of the device and its parasitic characteristics.

The same cost of a SCRIM device is currently around 800,000€, while the cost of a BPN device is about 2000€. These values are absolutely out of scale with respect to the system here set up. The comparison appears even more critical when operating costs are considered: 1) a SCRIM device needs personnel, periodic calibrations, and high operating costs, while the system herein set up has negligible or null operating costs. 2) A British pendulum test is not a high-speed device, it is time consuming, and about 0.5-1 hour are needed to carry out a measurement that refers to about 100 meters along a straight line of a road section.

The **pros** of the system include the fact that it is low cost, parasitic (uses common vehicles), low cost, born to be connected (V2X), and better spans across time (quasi-continuous monitoring) and space (the wandering of wheel trajectories implies that the monitoring practically refers to all the point of the carriageway). This point is crucial because of the possibility to detect:

- Long-term, structural changes in the hysteretic friction of rubber or in the resistance force due to rubber-pavement adhesion or in the cohesion bond force of the interface contaminant or in the drag force of air and fluid if fluid is present on the pavement surface).

TABLE 2. Design of experiments and average friction.

Surface	Main Braking manoeuvres	f_{MEAS} (average friction -EN13036-4)
1	FR1_1 to FR1_13	55
2	FR2_14 to FR2_16	46
3	FR3_17 to FR3_25	54

- Short-term changes due to unexpected spills (e.g., diesel or oil or other contaminants), snow, and ice, with immediate consequences in terms of smaller friction coefficient, longer stopping distances and lower longitudinal gradients needed for a vehicle to start.
- Both the points above are vital because of the intrinsic difficulties that the common systems for friction monitoring (e.g., SCRIM) undergo with respect to the need for high sampling frequencies, where high costs for buying the devices and for conducting the monitoring hinder the possibility to manage high-frequency monitoring with reasonable budgets.

At the same time, the following **contras** should be emphasised for the sake of clarity: it doesn—t provide certified values for the sake of acceptance procedures, where the pavement undergoes acceptance procedures and tests prior to the acceptance, and possible penalties (pay adjustments) need to be quantified. This means that its use in contract litigations appears unprobable. Another problem refers to its dependency on the driver and vehicle. Indeed, friction depends on a number of factors and on driving behaviour, tyre characteristics and wear, vehicle characteristics and age, among others, impact the braking process and the decelerations. Another issue pertains to the reliability of the measurements, which could also depend on the systems used and the quality of the electronic components. Finally, like the competing systems, there could be ethical/security issues because this would be a widespread, user-centred system, and these devices could be hacked, leading to traffic management problems.

Taken together, the analysis above points out that the system is low cost and has outstanding potential, but its use appears more as a safety-, risk-, and maintenance-related system for highways and streets under operation than as a device to perform acceptance procedures.

V. DESIGN OF EXPERIMENTS AND RESULTS

Table 2 summaries the surfaces and the braking processes analysed in order to implement and validate the system. We recall that the performance of each surface depends on the characteristics of the asphalt, directly influencing braking capacity and tyre-pavement friction [35]. Therefore, it is essential to validate our model on different surfaces to ensure reliable results in real-world scenarios.

The same vehicle instrumented with the system herein set up, was used to gather and monitor dataset for three given surfaces. For each surface, the friction along the vehicle path was preliminarily measured using the British Pendulum Tester according to EN13036-4. It is noted that the friction coefficient is highly dependent on the boundary conditions. The EN13036-4 is supposed to refer to $50km/h$ (cf. [36]), patterned tyres, locked wheels, on a wet road (cf. [37]; [38]) while contract specifications usually refer to the SFC measured by the SCRIM (cf. [39]) and BS 7941-1 (cf. [40]).

In turn, the Italian national standard for road design does not specify which device the design friction values refer to.

Figure 7 illustrates the results obtained through the new system. Note that the X-axis refers to speed (m/s) while the Y-axis refers to the friction coefficient. Different colours refer to different records; specifically, each colour corresponds to the estimated coefficient of friction during each braking in the Dataset. Records were collected while driving on an urban road, reaching a maximum speed of 70 km/h within the imposed speed limits.

The friction coefficient values were obtained with both moderate and aggressive driving style. The maximum values of the coefficient of friction were calculated during aggressive braking, for example in the FR1_1 braking of about 15s duration (best shown in 9c), decreasing the speed from 56 to 7.2 km/h.

Based on the international literature and standards, it is expected that the available (maximum) friction coefficient decreases when speeds increase. As an example, Figure 7 reports the friction coefficient versus speed for surfaces 1 and 2 according to both the longitudinal friction coefficient used in the Italian standard (DM6792/01) (black dashed line) and experimental results. In this paper for brevity, we call the friction curve given in the DM6792/01 standard with the term ‘‘theoretical limit curve’’.

The results are displayed in the plot, in which the estimated friction coefficient pavement-tyre is related to vehicle speed. This point cloud is always below the theoretical limit curve, indicating that the method accurately captures realistic friction levels experienced during various driving scenarios, e.g., gentle deceleration, moderate braking, and emergency stop. It is evident that the obtained estimation values show a significant dependence on the nature of braking. In fact, during hard braking, the estimated coefficients approach the theoretical maximum, indicating a greater degree of pavement-tyre interaction and greater use of available friction. This indicates that the estimation method is sensitive to changes in the deceleration rate, i.e., the driver’s driving style during braking. Lower values of the friction coefficient, particularly those well below the theoretical limit, may indicate both a conservative driving style, resulting in the event of gentle braking, but may also reflect pavement-tyre interaction under less demanding conditions.

This demonstrates both the method’s sensitivity to dynamic changes and its robustness in identifying changes in deceleration rates.

In fact, in scenario 1, hard braking reached the limit value. As highlighted in Figure 8, on several occasions, the braking

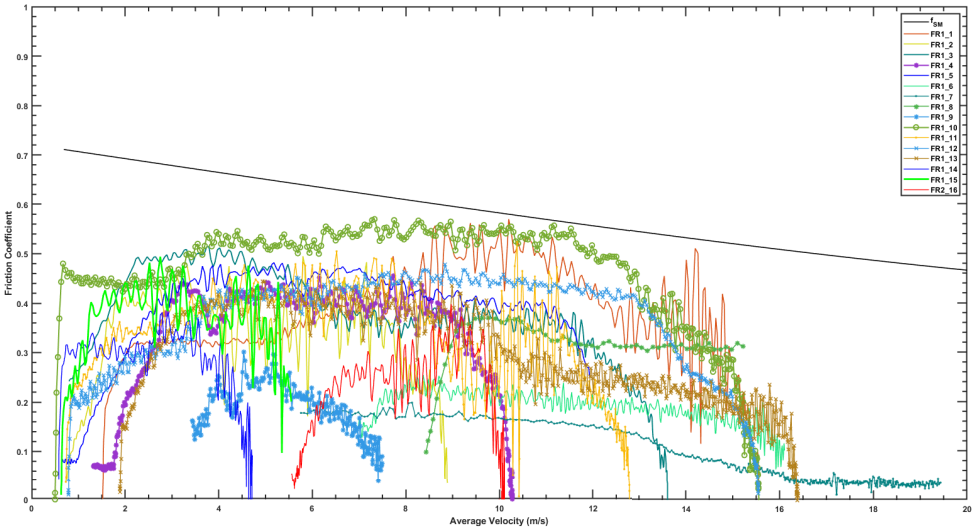

FIGURE 7. Braking processes on surfaces 1 and 2.

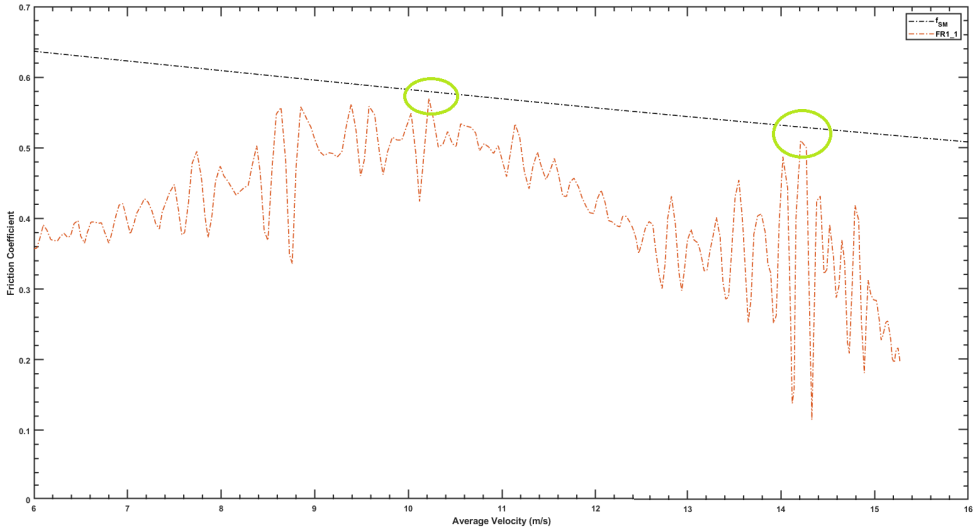

FIGURE 8. Focus on one of the hard braking events recorded in the Dataset.

process required a high coefficient of friction on the paved road. Thus, the interaction between the characteristics of the pavement and the tyre made it possible to maintain control of the vehicle even under intense braking conditions.

Another characteristic of each record is its bell-shaped trend. The rationale behind this depends on the fact that at the beginning of the braking process, the friction used (which is lower than the one available) is quite low, while in the median part of the process, a higher friction coefficient is needed. Finally, the final part of the braking process involved lower friction coefficients. Hence, for the single record, higher speeds correspond to the start of the braking process and vice versa.

Figure 9a to 9h illustrate how friction (Y-axis) and speed (expressed in m/s and reduced by a factor of 1/25, Y-axis) vary as a function of time (expressed in s, X-axis) in eight scenarios (surfaces 1 and 2). Braking manoeuvres in tangents are considered.

Each graph is related to a deceleration. Each deceleration, shown on the time axis (X-axis), is represented by the velocity (blue line) and estimated coefficient of friction (orange dots), for the duration of the observed phenomenon. Each deceleration has its own time interval. Specifically, the decelerations shown in the figure have durations ranging from 5s to 1.5s. The type of friction course is different: the first six figures are associated with asphalt pavement (surface 1), while the last two refer to an unpaved road (surface 2).

The speed over time decreases. The absolute value of its first derivative decreases, too. For each curve/event, the corresponding Jerk appears positive, and values in the

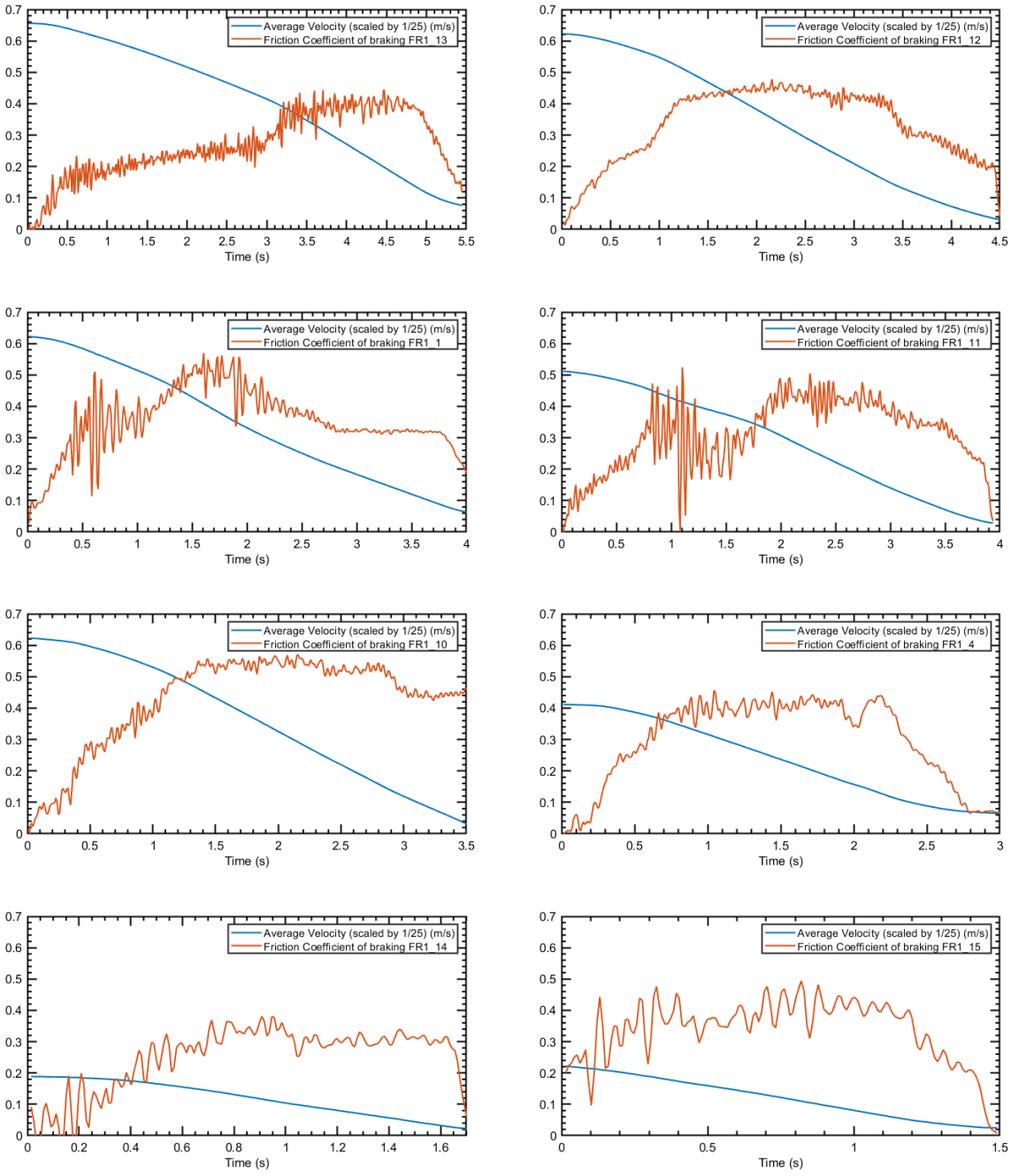

FIGURE 9. Breaking processes for surface 1 and surface 2.

range 0.23-0.65 m/s^3 are given. These values appear quite comfortable for seated occupants (<0.9-3.6 m/s^3, [41]). The corresponding friction coefficient undergoes three main steps:

1) Increasing branch (where speed decreases and friction increases). Here, friction gain ranges from about 0.05 to about 0.2;
2) Decreasing branch (where the friction and the speed decrease). In this case, the friction decrease is usually higher than the corresponding increase;
3) One or more arcs in which the friction is quite stable and the speed decreases. In this case, this steady state usually lasts less than 3s.

The speed evolution over time shows that the solicitations induced on the vehicle are mostly regular, in some cases uniform over time. However, even under these non-limiting conditions, it is possible to record the vehicle's response. In fact, the trend of the estimated coefficient of friction over time shows how each increase in the demand for braking force (i.e., when greater decelerations are detected), corresponds

to a peak in the estimated coefficient of friction. In this case, each demand for grip by the vehicle corresponds to a corresponding grip available on the road surface.

Figure 10 compares the friction coefficient as a function of average speed for two braking events: one on surface 1 (blue curve, FR1_4) and the other on surface 2 (green curve, FR2_16). The dashed black line represents the theoretical limit curve f_{SM} based on the DM6792/01 standard. Both events start from the same initial speed, about 10 m/s, and exhibit similar behaviour during the final phase of braking, i.e., there is a progressive reduction of the coefficient until it reaches zero.

In contrast, during the initial phase, both curves observe an increase in the friction coefficient, but in different ways. The coefficient of friction for surface 2 shows a slow rise along the y-axis, suggesting that surface 2 takes a longer time to reach its peak coefficient of friction. This slower rise could be due to the physical properties of surface 2, which may offer a less immediate response at the beginning of the braking process. On the other hand, surface 1 shows a steeper and faster rise in friction, indicating a faster response and a more immediate and powerful interaction between the tyre and the pavement.

Moreover, in the middle part of the graph, the curves show distinct behaviours as speed changes, showing a significant difference between the two surfaces. In particular, during braking FR1_4 shows more stable behaviour and a higher coefficient of friction than FR2_16. The consistently higher friction values of surface 1 result in safer braking performance, reducing the risk of skidding and ensuring braking stability.

Figure 11 refers to an asphalt concrete located in Reggio Calabria (surface 3). In particular, it is a plot of the friction coefficient (Y-axis) *versus* the speed (X-axis). Importantly, it reports also

1) The theoretical limit curve (dashed black line). This refers to the friction curve stated in the standard DM6792/01 for motorways, whose approximate equation is

$$f_{SM} = -0.011950v + 0.706836 \tag{2}$$

where v stands for speed in m/s.

2) The plot of the experimental results collected at Reggio Calabria.

In Figure 12 (surface 3), the X-axis reports time in seconds, while the Y-axis reports the following data gathered through the onboard device:

- The acceleration in percentage ($a\%$):
- The speed in percentage ($v\%$);
- The longitudinal friction coefficient in percentage ($f\%$);
- In the same plot, at the given instant, t, for the given speed, v,the corresponding standard friction ratios for rural roads (longitudinal friction as per the Italian Decree 6792/01) and for motorways (same standard) are reported (cf. $f\%_{SR}$ and $f\%_{SM}$, respectively). While the approximate equation of f_{SM} is reported above and has a maximum of about 0.7, for f_{SR} it is

$$f_{SR} = -0.009556.v + 0.519681 \tag{3}$$

where the maximum is about 0.5.

This result points out what follows:

- There are three different phases, i.e., a first phase where the speed decreases, the absolute value of the deceleration increases, and the friction follows the same trend as for the deceleration (increase). This phase has a duration of about 0.5 seconds. During the second phase, while the speed continues to decrease, both $f\%$ (the estimated friction) and $a\%$ undergo a slight increase. Importantly, not only do they superpose each other, but they also superpose with $f\%_{SR}$ and $f\%_{SM}$. A third phase, where, while the speed is approaching zero, both f% and a% decrease quite suddenly.
- While the duration of the first phase (a sort of transitory phase) lasts about 0.5s and the third phase lasts for about 0.1s, the second phase lasts about 1.8s with a slight increase of f% and a% and a sort of steady state. Though this, it basically represents a sort of steady state.
- Given that the scenario taken into consideration refers to a rural road, the system herein set up allows for assessing that the friction demanded (herein measured, i.e., f, cf. the plot on the right) is higher than the design friction (f_{SR}). This result is crucial and demonstrates that such an assessment would provide the road agency with a parasitic (without ad-hoc investigations) and continuous (because many vehicles would provide for many assessments per day) monitoring, where the consequences in terms of pavement management would be vital.
- Additionally, in the specific case, the friction derived through the on-board system is somehow higher than the f_{SM}, which introduces a further safety coefficient in terms of pavement management system (PMS).
- To this end, it seems noteworthy to highlight that this tool has a multi-fold application because it refers to different procedures, circumstances and phases during the life cycle of a road system, that is to say:
  - The acceptance phase, where the acceptance procedures are carried out (QA/QC procedures, cf. [42]) to assess if the as-built pavement complies with the contract specifications.
  - The operation phase (after the acceptance procedures were carried out), where three main domains of pavement lifecycle are given (cf. [43]; [44]):
    A) f is above the so-called investigatory level, IL. In this case the road agency does not experience any concerns.
    B) f is below the IL and above the threshold level, TL. In this case the road agency should complement the parasitic systems with more traditional high-speed monitoring systems (e.g., Sideway force coefficient routine investigation machine, SCRIM).

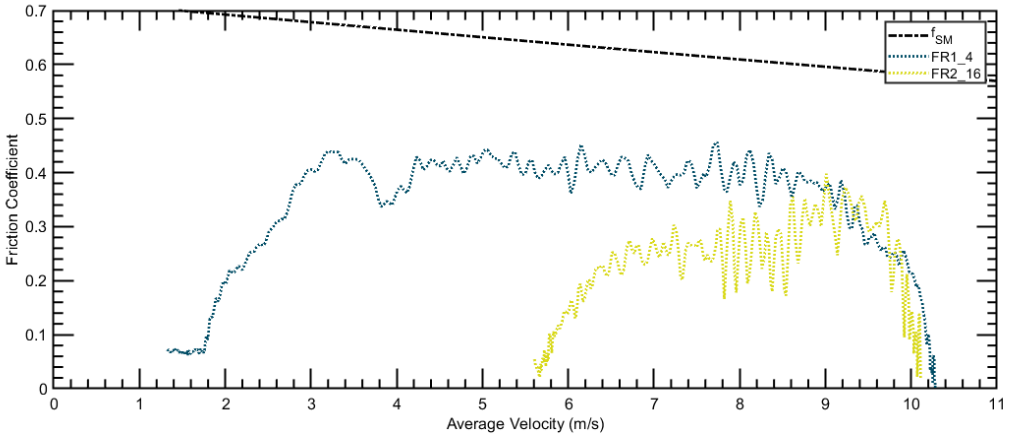

FIGURE 10. Comparing braking FR1_4 and FR2_16 that pertain to surface 1 and 2, respectively.

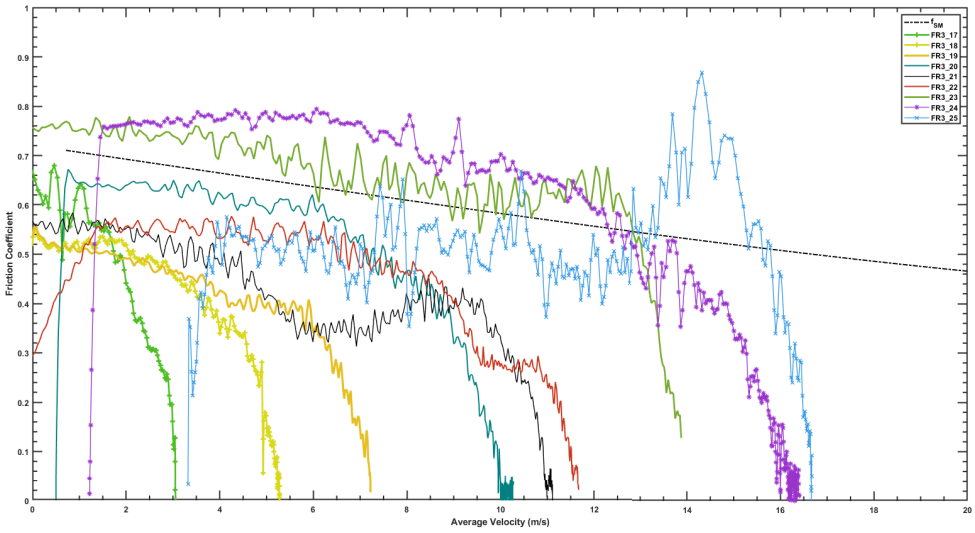

FIGURE 11. Braking processes for surface 3.

C) f is below TL, where the road agency should close the road to the traffic or introduce a different posted speed.

– Because acceptance procedures are project specific (they are based on contract specifications), and this applies to the design parameters (such as f_{SR} and f_{SM}) and IL and TL, this calls for a further step and a further need, that is to say the georeferencing of the plot, so that once the on-board system produces data and these data are sent to the road agency (as data or plots), these data are connected to the corresponding geodata, that allow for deriving the right contract specifications (for acceptance procedures) and the right IL and TL (based on the type of road and on the location (e.g., approaches to railway crossings, where higher friction levels are required, or undivided carriageways – event free, where lower levels are allowed, (cf. [44]).
– Importantly, such a system would allow for a crucial multipurpose and comprehensive tool where
1) different speeds can be compared based on the actual friction "offer" and based on the actual percentage of autonomous vehicles, e.g., inferred design speed, design speed, operating speeds, statutory speed limits, and posted speeds (cf. [45]).
2) Different friction "types" can be analysed versus the actual measurements (e.g., IL-related, TL-related, and acceptance-related).

- Comparing Figure 11 and Figure 7 it is possible to observe that the level of friction demanded (the one assessed through the system) is quite different. To this end, it is noted that while Figure 11 (surface 3), the driver was quite young (male, 30 years old), for Figure 7 (surfaces 1 and 2), the driver was quite elder (male, 68 years old). This points out that the system should/could be complemented with other pieces

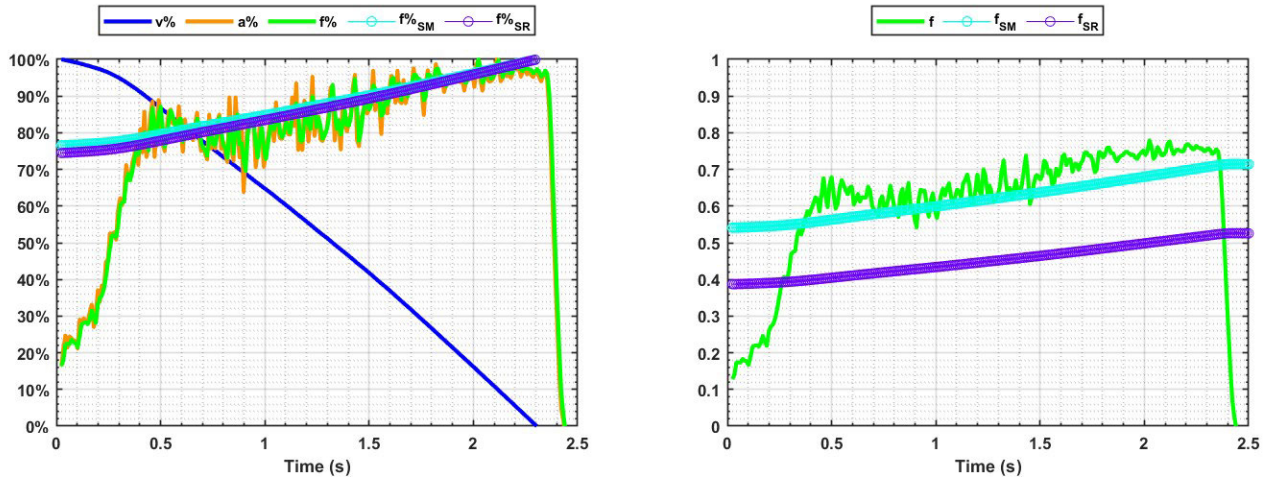

FIGURE 12. Braking number 23 on surface 3 (FR3_23).

of information related to the age of the driver and possibly to his/her gender as well as the type of vehicle (autonomous versus non-autonomous, cf. [46]; [47]), where, when assessing the maximum friction, the statistical weight of teen/adults, male/female, and autonomous and nonautonomous vehicle could be different).

By referring to the case plot in Figures 13a and 13b (surface 3), the scenario seems to include two different processes and in between a sort of slippage process:

- First braking process. During the first braking process, there are still three phases:
  1) Sudden increase of acceleration and demanded friction (about 0.5s).
  2) Quasi-steady phase (about 2s).
  3) Steep decay of friction demanded.
- Slippage and/or end of the braking effort. Importantly, after about 3 seconds (when the friction offered by the pavement is negligible), the speed is substantially different from zero (about 20% of its peak).
- Second braking process. This state (speed different from zero and quasi-null friction) refers to a friction loss for low speeds and is followed by a second braking process. This latter has the first and third phases that are very brief, while the second phase lasts for about 1.5 seconds.

Instead, the scenario in Figures 14a and 14b (surface 3) includes several processes:

- Initial phase. Initial phase with null acceleration: an initial phase of constant velocity with the duration of 1s is shown in the graph. In this null deceleration interval, no surface friction is required and, therefore, the coefficient of friction is in the lower left part of the graph, slightly above 0%.
- Second phase. Deceleration and friction increase phase: in the second phase, the decrease in speed occurs, and then the corresponding increase in deceleration leads the friction curve to rise. The friction coefficient rises until it follows (and later exceeds) the trend of the f_{SM} and f_{SR} curves. The duration of this interval is about 2.5s, with the point of intersection (and subsequent exceedance) between the curves occurring after about 1.5s from the instant of the beginning of the interval.
- Third and last phase. End of braking and speed recovery: around the 4-second mark, the braking effort ends after reducing the speed by 90% from the initial constant value. In this last phase, the speed slowly begins to increase again, and, consequently, the coefficient of friction decreases suddenly, returning to approximately zero, as in the initial phase.

In Tables 3 and 4 a tentative implementation of the method herein set up, implemented and validated is proposed, where the monitored friction is compared with standards (f_{SR}), investigatory levels (IL) and threshold levels (TL) with the aim to provide autonomous vehicles (V2V, V2I, I2X), drivers (V2V and V2X, V2I, I2X), road agencies (V2RA, I2X), and remaining stakeholders (e.g., police, ambulances, and medical emergencies and services) with crucial and timeliness information (cf. Figure 15).

To this end it is noted that:

Starting from these outputs, the expected types of communication refer to V2RA (vehicle to road agency, via V2I), V2I (vehicle to infrastructure, including variable message signs, arrow boards, electronic highway message boards, and traffic signs), V2V (vehicle to vehicle). At the same time, the expected types of action include

1) ILT (triggering of investigatory level, with increase of the frequency of routine investigations, e.g., by using the SCRIM machine).
2) TLT (triggering of the threshold level).
3) M&O: mill and lay down of a new layer.
4) O: overlay.
5) BT: bituminous treatment.

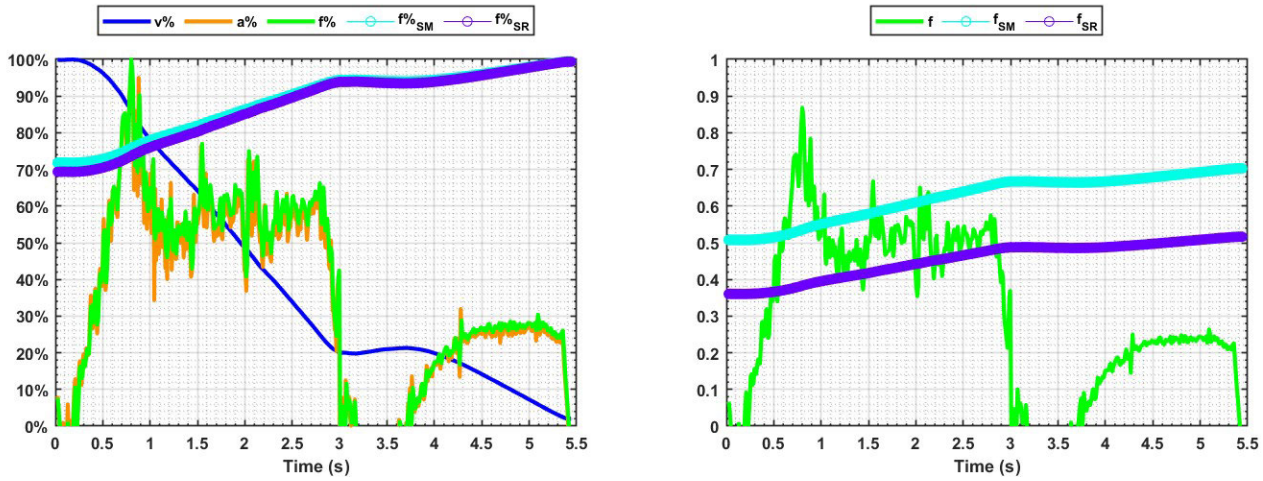

FIGURE 13. Braking number 25 on surface 3 (FR3_25).

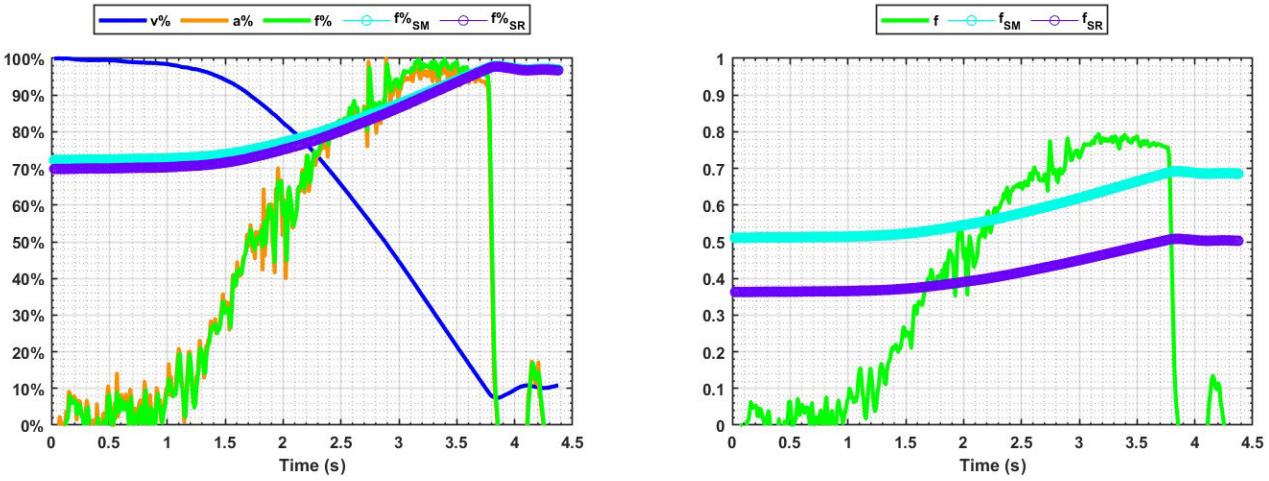

FIGURE 14. Braking number 24 on surface 3 (FR3_24).

TABLE 3. From system data to expected actions (part 1).

Braking events	Max friction ($f_{max}(v)$)	v(m/s)	$f_{max}(v)/f_{SR}(v)$	$f_{max}(v)$/IL	$f_{max}(v)$/TL
FR1_1	0.57	10.2	1.36	1.43	1.90
FR1_2	0.49	5.8	1.10	1.20	1.65
FR1_3	0.51	3.8	1.04	1.30	1.70
FR1_4	0.46	7.7	1,02	1,15	1.53
FR1_5	0.48	5.2	1.02	1.20	1.60
FR1_6	0.25	8.37	0,56	0,57	0,83
FR1_7	0.19	8.13	0.43	0.45	0.63
FR1_8	0.36	9.62	0.83	0.90	1.20
FR1_9	0.30	4.53	0.62	0.75	1.00
FR1_10	0.57	7.33	1.30	1.42	1.90
FR1_11	0.52	10.38	1.23	1.30	1.73
FR1_12	0.48	8.84	1.10	1.20	1.60
FR1_13	0.44	7.91	1.00	1.10	1.46
FR2_14	0.38	4.42	0.80	1.20	1.27
FR2_15	0.49	2.75	1.00	1.22	1.63
FR2_16	0.39	9.97	0.91	0.91	1.30

TABLE 4. From system data to expected actions (part 2).

Braking events	Max friction ($f_{max}(v)$)	v(m/s)	$f_{max}(v)/f_{SR}(v)$	$f_{max}(v)$/IL	$f_{max}(v)$/TL
FR3_17	0.68	0.46	1.30	1.70	2.30
FR3_18	0.55	0.10	1.10	1.40	1.80
FR3_19	0.56	0.10	1.10	1.40	1.90
FR3_20	0.67	0.76	1.13	1.70	2.30
FR3_21	0.58	0.86	1.13	1.45	2.00
FR3_22	0.58	4.71	1.23	1.45	2.00
FR3_23	0.78	2.07	1.56	2.00	2.60
FR3_24	0.79	6.07	1.73	2.00	2.60
FR3_25	0.87	14.32	2.30	2.18	2.90

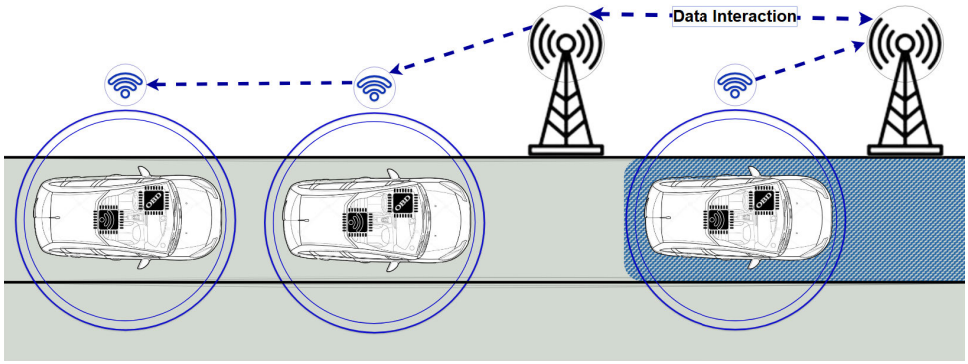

FIGURE 15. V2X for friction purposes.

6) SR: speed reduction or/and traffic deviation or/and traffic closure).

The comparison between the friction level derived through the system herein set up and IL and TL levels was tentatively derived based on (cf. [48]).

VI. CONCLUSION AND FUTURE WORK

A. TECHNICAL CONTRIBUTIONS SUMMARY

The main technical contributions of this study can be summarised as follows:

- the development and deployment of a low-cost, parasitic friction estimation system fully integrated into existing on-board hardware without requiring cloud or auxiliary infrastructure;
- the implementation of a physics-based algorithm for estimating the friction coefficient $f(V)$, designed to run on a resource-constrained STM32 microcontroller with real-time processing capabilities;
- the design of an interrupt-driven data acquisition and fusion pipeline combining accelerometer, gyroscope, and OBDII vehicle speed data via UART communication;
- performing experimental validation, including different road surfaces and braking styles, and comparing the results obtained with standard reference curves and critical friction thresholds (IL, TL).

B. FINAL REMARKS AND DEVELOPMENT PERSPECTIVES

Based on the tests and analyses, the following conclusions can be drawn:

- Multiple research gaps call for setting up parasitic methods and technologies for friction monitoring during traffic operations.
- To this end, in this study, a system was designed, set up, and implemented to gather friction-related information, starting from on-board devices already existing in common vehicles.
- Based on the data gathered, friction can be derived for each breaking manoeuvre, using the algorithms implemented on on-board devices.
- Data can be compared with reference curves and with on-site measurements carried out using traditional methods.
- The system is low cost and has outstanding potential, but its use appears more as a safety-, risk-, and maintenance-related system for highways and streets under operation than as a device to perform acceptance procedures. These latter, having an economic purpose (pay adjustment), could be carried out through standardized methods as mentioned above.
- There are several advantages of the (data-driven) model introduced and validated in this study. Indeed, the approach herein introduced and validated allows for the accurate estimation of the tyre-pavement friction

coefficient using a direct method, and sensors were integrated into the on-board system, thus avoiding the use of external sensors. The presented system is, therefore, the result of the trade-off between cost and estimation accuracy.
- In addition, the set-up implements a real-time model, that is, it has the ability to respond in a timely manner. This is an advantage, especially in critical conditions where timely response is the key to preventing accidents.
- In conclusion, the integration into the vehicle and real-time response make this set-up preferable to space-intensive and static solutions.
- Several limitations of this study still remain. They refer to the number of sets of braking manoeuvres, the optimisation of the hardware and software of the system to add to the on-board system of vehicles (autonomous or nonautonomous), and the need for a systematic comparison between the data values recorded with this system and the ones that derive from other systems for friction measurement.

Future developments will focus on various aspects aimed at improving the system:

- Software Adaptation: To further enhance the versatility and applicability of the developed system, it is essential to adapt the software to the various standard communication protocols used by vehicles. This update will enable the system to interface with a broader range of control units, significantly increasing the number of compatible vehicle models.
- Hardware Optimization: On the hardware side, advancements will focus on designing a portable solution to reduce the physical footprint of the system and facilitate widespread adoption. This entails integrating all components, including sensors and the Wi-Fi module, into a single compact board.
- Energy Efficiency: To address energy consumption challenges, the implementation of low-power modes during non-critical tasks will be prioritized, along with the adoption of computationally optimized algorithms.
- Dataset Expansion: Another key area of improvement involves expanding the experimental campaign to test the proposed system across a wider spectrum of operational conditions. This includes conducting tests with tyres exhibiting varying levels of wearing under different atmospheric conditions and on diverse pavement types beyond those considered in this work. By significantly increasing the number of tests and the diversity of operational scenarios (including surfaces), the aim is not only to refine the proposed setup but also to create a comprehensive and robust dataset, which will be critical for the subsequent development phases.
- Edge Machine Learning Integration: An innovative solution involves the adoption of Edge Machine Learning (EdgeML) algorithms, enabling the system to continuously improve the prediction accuracy of the friction coefficient. This will require the definition of both a lightweight ML model optimised for edge devices and a suitable method for training the model. This advancement will empower the setup to:
  - Dynamically adapt to varying operating conditions, such as weather changes and pavement variations.
  - Customize predictions based on the driver's specific driving patterns and the unique characteristics of each vehicle.

  This will ensure real-time predictions that are highly accurate and tailored to specific scenarios.
- Systematic Validation: Future developments will also include a systematic validation process, where data collected by the proposed system will be compared with results from well-established friction measurement technologies.
- The trend analysis of the friction coefficient provides an opportunity to study a possible relationship between driving behaviour and the demographic characteristics of drivers, including age and gender. In fact, it will be crucial to investigate how, just by examining the graphs (particularly $f(v)$), the difference in friction demand among different drivers can suggest the existence of parameters that may link braking dynamics with both driving style and potentially driver characteristics. This study is particularly relevant since it will enable the addition of new details in road safety assessment in order to accomplish with an automatized and reliable classification of driver profiles based on the friction coefficient curve. Thus, this and future studies aim to contribute to the development of intelligent transportation systems by improving their quality, customization and safety.

Combined, these advancements aim to validate the proposed approach to meet the demands of modern vehicular environments, while ensuring robustness, scalability, compatibility, and introducing innovative capabilities.

ABBREVIATIONS

The following abbreviations are used in this manuscript:

ABS	Anti-lock braking system
AT Command	Attention Command
AV	Autonomous Vehicles
CAN	Controller Area Network
DOT	Departments of transportation
ECU	Electronic Control Unit
EdgeML	Edge Machine Learning
EOBD	European On-Board Diagnostics
ESC	Electronic stability control
HDV	Human-Driven Vehicles
I^2C	Inter-Integrated Circuit
IL	Investigatory Levels
IMU	Inertial Measurement Unit
MCU	Microcontroller
m/s^2	The unit of measurement of acceleration

mg	milli G-forces, the unit of measurement of acceleration
OBD	On-Board Diagnostics
PID	Parameter ID
PMS	Pavement Management System
PWM	Pulse Width Modulation
SD	Secure Digital
TCS	Traction control systems
TL	Threshold Levels
TRFC	Tyre Road Friction coefficient
USART	Universal Asynchronous Receiver-Transmitter
V2I	Vehicle to Infrastructure
V2RA	Vehicle to road agency
V2V	Vehicle to vehicle
V2X	Vehicle-to-everything Communication
VPW	Variable Pulse Width

ACKNOWLEDGMENT

The authors would like to thank all who sustained them with this research.

REFERENCES

[1] P. Cairney and P. Hillier, "Understanding vicroads" skid resistance investigatory levels," VicRoads, Denmark, KV, Australia, Tech. Rep. TN111, Nov. 2018

[2] J. Hall, K. L. Smith, L. Titus-Glover, J. C. Wambold, T. J. Yager, and Z. Rado, "Guide for pavement friction," Transp. Res. Board (TRB), Washington, D.C, USA, Final Rep. NCHRP Project 1, 2009, p. 43.

[3] T. Andriejauskas, V. Vorobjovas, and V. Mielonas, "Evaluation of skid resistance characteristics and measurement methods," in *Proc. Environ. Eng. Int. Conf. Environ. Eng. (ICEE)*, Jan. 2014, p. 1.

[4] C. G. Wallman and H. Astrom, "Friction measurement methods and the correlation between road friction and traffic safety: A literature review," Swedish Nat. Road Transp. Res. Inst. (VTI), Linköping, Sweden, Tech. Rep. SE-581 95, 2001.

[5] M. Liu, "Design of traffic-signal progression for the modern streetcar: Case study of Qilin line one, Nanjing, China," *J. Transp. Eng., A, Syst.*, vol. 147, no. 12, pp. 1–14, Dec. 2021, doi: 10.1061/jtepbs.0000603.

[6] S. K. Jayaraman, C. Creech, D. M. Tilbury, X. J. Yang, A. K. Pradhan, K. M. Tsui, and L. P. Robert, "Pedestrian trust in automated vehicles: Role of traffic signal and AV driving behavior," *Frontiers Robot. AI*, vol. 6, p. 117, Nov. 2019.

[7] K. B. Singh, M. A. Arat, and S. Taheri, "Enhancement of collision mitigation braking system performance through real-time estimation of tire-road friction coefficient by means of smart tires," *SAE Int. J. Passenger Cars Electron. Electr. Syst.*, vol. 5, no. 2, pp. 607–624, Sep. 2012.

[8] G. Schiaffino, L. G. Del Pizzo, S. Silvestri, F. Bianco, G. Licitra, and F. G. Praticò, "Machine learning techniques applied to road health status recognition through tyre cavity noise analysis," *J. Phys., Conf. Ser.*, vol. 2162, no. 1, Jan. 2022, Art. no. 012011.

[9] J. Granlund, "Slipperiness on contaminated road surfaces—Diesel and loose gravel on bare asphalt," Sveriges MotorCyklister, Borlänge Sverige, Dalarna, Sweden, doi: 10.13140/RG.2.2.29956.22407.

[10] J. Wang, L. Alexander, and R. Rajamani, "Friction estimation on highway vehicles using longitudinal measurements," *J. Dyn. Syst., Meas., Control*, vol. 126, no. 2, pp. 265–275, Jun. 2004.

[11] Y. Wang, J. Hu, F. Wang, H. Dong, Y. Yan, Y. Ren, C. Zhou, and G. Yin, "Tire road friction coefficient estimation: Review and research perspectives," *Chin. J. Mech. Eng.*, vol. 35, no. 1, p. 6, Dec. 2022.

[12] R. Ghandour, A. Victorino, M. Doumiati, and A. Charara, "Tire/road friction coefficient estimation applied to road safety," in *Proc. 18th Medit. Conf. Control Autom. (MED)*, Jun. 2010, pp. 1485–1490.

[13] K. B. Singh and S. Taheri, "Estimation of tire–road friction coefficient and its application in chassis control systems," *Syst. Sci. Control Eng.*, vol. 3, no. 1, pp. 39–61, Jan. 2015.

[14] F. Gustafsson, "Slip-based tire-road friction estimation," *Automatica*, vol. 33, no. 6, pp. 1087–1099, Jun. 1997.

[15] K. B. Singh and S. Sivaramakrishnan, "Extended pacejka tire model for enhanced vehicle stability control," 2023, *arXiv:2305.18422*.

[16] C. Ahn, H. Peng, and H. E. Tseng, "Robust estimation of road friction coefficient using lateral and longitudinal vehicle dynamics," *Vehicle Syst. Dyn.*, vol. 50, no. 6, pp. 961–985, Jun. 2012.

[17] S. Müller, M. Uchanski, and K. Hedrick, "Estimation of the maximum tire-road friction coefficient," *J. Dyn. Syst., Meas., Control*, vol. 125, no. 4, pp. 607–617, Dec. 2003.

[18] R. Rajamani, N. Piyabongkarn, J. Lew, K. Yi, and G. Phanomchoeng, "Tire-road friction-coefficient estimation," *IEEE Control Syst. Mag.*, vol. 30, no. 4, pp. 54–69, Aug. 2010.

[19] Y. Ren, "Modelling and control of narrow tilting vehicle for future transportation system," in *Intell. Efficient Transport Syst.*, vol. 133. London, U.K.: IntechOpen, Apr. 2020, p. 133.

[20] R. Van Der Steen, "Tyre/road friction modeling: Literature survey," Technische Universiteit Eindhoven, Tech. Rep. DCT rapporten, vol. 72, 2007.

[21] S. Andersson, "Friction and wear simulation of the wheel–rail interface," in *Wheel–Rail Interface Handbook*. Amsterdam, The Netherlands: Elsevier, 2009, pp. 93–124.

[22] H. Olsson, K. J. Åström, C. Canudas de Wit, M. Gäfvert, and P. Lischinsky, "Friction models and friction compensation," *Eur. J. Control*, vol. 4, no. 3, pp. 176–195, Jan. 1998.

[23] M. Schuderer, G. Rill, T. Schaeffer, and C. Schulz, "Friction modeling from a practical point of view," *Multibody Syst. Dyn.*, vol. 63, nos. 1–2, pp. 141–158, Feb. 2025.

[24] L. Li, J. Song, H.-Z. Li, D.-S. Shan, L. Kong, and C. C. Yang, "Comprehensive prediction method of road friction for vehicle dynamics control," *Proc. Inst. Mech. Eng., D, J. Automobile Eng.*, vol. 223, no. 8, pp. 987–1002, Aug. 2009, doi: 10.1243/09544070jauto1168.

[25] J.-O. Hahn, R. Rajamani, and L. Alexander, "GPS-based real-time identification of tire-road friction coefficient," *IEEE Trans. Control Syst. Technol.*, vol. 10, no. 3, pp. 331–343, May 2002, doi: 10.1109/87.998016.

[26] B. Leng, D. Jin, L. Xiong, X. Yang, and Z. Yu, "Estimation of tire-road peak adhesion coefficient for intelligent electric vehicles based on camera and tire dynamics information fusion," *Mech. Syst. Signal Process.*, vol. 150, Mar. 2021, Art. no. 107275, doi: 10.1016/j.ymssp.2020.107275.

[27] S. D. Klein, "Friction estimation and detection for an electric power steering system," Patent 9 150 244 B2, Apr. 7, 2010. [Online]. Available: https://patents.google.com/patent/US9150244B2/en

[28] L. D. B. D. Bell, "Method and apparatus for monitoring the coefficient of friction between a tire and rolling surface, particularly to provide the vehicle operator with coefficient of friction, tire tread wear out and skid warning indications," U.S. Patent 5 864 056 A, Jan. 26, 1999. [Online]. Available: https://patents.google.com/patent/US5864056A/en

[29] C. Ahn, H. Peng, and H. E. Tseng, "Robust estimation of road frictional coefficient," *IEEE Trans. Control Syst. Technol.*, vol. 21, no. 1, pp. 1–13, Jan. 2013, doi: 10.1109/TCST.2011.2170838.

[30] L. Willemet, F. Roël, D. Abbink, I. Birznieks, and M. Wiertlewski, "Grip force control under sudden change of friction," *J. Physiol.*, vol. 603, no. 2, pp. 411–422, Jan. 2025, doi: 10.1113/jp286486.

[31] M. S. Shahriar, A. K. Kale, and K. Chang, "Enhancing intersection traffic safety utilizing V2I communications: Design and evaluation of machine learning based framework," *IEEE Access*, vol. 11, pp. 106024–106036, 2023, doi: 10.1109/ACCESS.2023.3319382.

[32] P. Baronti, P. Pillai, V. W. C. Chook, S. Chessa, A. Gotta, and Y. F. Hu, "Wireless sensor networks: A survey on the state of the art and the 802.15.4 and ZigBee standards," *Comput. Commun.*, vol. 30, no. 7, pp. 1655–1695, May 2007, doi: 10.1016/j.comcom.2006.12.020.

[33] M. Merenda, V. Mazzullo, M. Princi, A. Martino, R. Carotenuto, and D. Iero, "Evaluation of OBDII data contribution in tiny machine learning based driving behaviour monitoring," in *Proc. 7th Int. Conf. Smart Sustain. Technol. (SpliTech)*, Jul. 2022, pp. 1–6, doi: 10.23919/SpliTech55088.2022.9854360.

[34] *Advantech: OBDII Streamer Family*. Accessed: Oct. 30, 2024. [Online]. Available: https://advdownload.advantech.com/productfile/Downloadfile3/1-1I7 CBS8/BB-LD3IC-S_OBDII-Gateway-Gen3_Command&Response_r2_5019cr.pdf

[35] T. Singh, A. Patnaik, R. Chauhan, and A. Rishiraj, "Assessment of braking performance of Lapinus–Wollastonite fibre reinforced friction composite materials," *J. King Saud Univ. Eng. Sci.*, vol. 29, no. 2, pp. 183–190, Apr. 2017.

[36] P. D. Cenek, N. J. Jamieson, and R. J. Henderson, "Assessing road surface friction with the British pendulum tester in NZ," New Zealand Transport Agency (NZTA), Wellington, New Zealand, Tech. Rep. 73, 996. [Online]. Available: https://www.nzta.govt.nz/assets/resources/research/reports/073/073-Assessing-road-surface-friction-with-the-brittish-pendulum-tester-in-nz.pdf
[37] (1969). *Instructions for Using the Portable Skid-Resistance Tester, 2nd Edn. HMSO (Her Majesty's Stationery Office), London (1969). Road Note 27*. [Online]. Available: https://www.academia.edu/2628616/HMSO_Instructions_for_using_the_portable_skid_resistance_tester_2nd_edition_1969
[38] (1997). *Transport Research Laboratory (TRL): A Guide to Surface Dressing in Tropical and Sub-Tropical Countries. Technical Report Overseas Road Note 18*. Transport Research Laboratory (TRL). [Online]. Available: https://www.trl.co.uk/uploads/trl/documents/ORN018.pdf
[39] "QA specification R423 measurement of surface friction by sideways-force coefficient routine investigation machine (SCRIM)," NSW Roads Maritime Services, 2013.
[40] *Methods for Measuring the Skid Resistance of Pavement Surfaces—Part 1: Sideway-force Coefficient Routine Investigation Machine*. Accessed: May 29, 2025. [Online]. Available: https://knowledge.bsigroup.com/products/methods-for-measuring-the-skid-resistance-of-pavement-surfaces-sideway-force-coefficient-routine-investigation-machine?tab=history&version=standard
[41] K. Czarnecki, "Automated driving system (ADS) high-level quality requirements analysis—Driving behavior comfort," Univ. Waterloo, Waterloo, ON, Canada, 2018, doi: 10.13140/RG.2.2.19925.32483.
[42] F. G. Praticò and P. G. Briante, "Prediction of surface texture for better performance of friction courses," *Construct. Building Mater.*, vol. 230, Jan. 2020, Art. no. 116991.
[43] R. McCarthy, G. Flintsch, S. Katicha, E. D. L. Izeppi, and F. Guo, "Determining investigatory levels of friction with crash modelling," *Int. J. Pavement Eng.*, vol. 23, no. 9, pp. 3236–3243, Jul. 2022, doi: 10.1080/10298436.2021.1888089.
[44] (2012). *NZTA: NZTA T10 Specification: Specification for State Highway Skid Resistance Management. Technical Report, NZ Transport Agency*. [Online]. Available: https://www.nzta.govt.nz/assets/resources/skid-resistance-investigati on-treatment-selection/docs/skid-resistance-investigation-treatment-selection-2012.pdf
[45] S. He, F. Ding, C. Lu, and Y. Qi, "Impact of connected and autonomous vehicle dedicated lane on the freeway traffic efficiency," *Eur. Transp. Res. Rev.*, vol. 14, no. 1, p. 12, Dec. 2022.
[46] D. Kim, J. Park, S. Kim, and E. J. Soo, "Robust adaptive autonomous braking control for intelligent electric vehicles," *IFAC-PapersOnLine*, vol. 56, no. 2, pp. 11821–11826, 2023, doi: 10.1016/j.ifacol.2023.10.580.
[47] S. H. Teo and L. M. Gan, "Speeding driving behaviour: Age and gender experimental analysis," *MATEC Web Conf.*, vol. 74, p. 30, Jan. 2016.
[48] F. G. Praticò, "Impact of pavement friction decay on speed limits and autonomous vehicles: A theoretical and experimental study," *J. Road Eng.*, vol. 5, no. 1, pp. 35–47, Mar. 2025.

ALESSIA LAZZARO received the master's degree in electrical and electronics engineering from the University "Mediterranea" of Reggio Calabria (UNIRC), Italy, in 2024.

Her academic journey focused on the integration of TinyML and embedded systems, aiming to explore how machine learning can be efficiently implemented in hardware-limited environments. Her research interests include the practical applications of TinyML in improving the performance and capabilities of embedded devices. She contributes to the evolving field by addressing the challenges of deploying AI in resource-constrained settings, striving for innovation in energy efficiency, and processing power.

MASSIMO MERENDA (Member, IEEE) received the bachelor's, master's, and Ph.D. degrees in electronic engineering from the University "Mediterranea" of Reggio Calabria (UNIRC), Italy, in 2002, 2005, and 2009, respectively.

From 2003 to 2005, he was a fellow with the Institute of Microelectronics and Microsystems, Italian National Research Council (IMM-CNR), Naples, Italy. From 2011 to 2018, he was a Postdoctoral Researcher with UNIRC. From 2018 to 2021, he was a Researcher with the Department of Information Engineering, Infrastructure, and Sustainable Energy (DIIES), UNIRC, and the National Inter-University Consortium for Telecommunications (CNIT). From 2021 to 2022, he was a Senior Scientist with the Cooperative Digital Technologies Competence Unit, Austrian Institute of Technology (AIT), Vienna. Since October 2022, he has been a Senior Researcher with DIIES, UNIRC. His main research interests include the design of CMOS IC, silicon sensors, energy harvesting, RFID smart tag and applications, embedded systems, the Internet of Things (IoT), and edge computing for applications of the Internet of Conscious Things.

FILIPPO GIAMMARIA PRATICÒ received the Laurea degree (Hons.) in civil engineering from the University of Pisa, and the Ph.D. degree in transportation infrastructures from Palermo University. After his industrial occupation with the University Mediterranea of Reggio Calabria, he became an Associate Professor, in 2002, and habilitated full in 2012 call. He is currently the Deputy Director of the master's school and the DIMET Department, and the Director of the Road Laboratory. He is a member of the TRB of U.S. National Academies, and the chair of several international committees, involved in national and international research/industrial projects. He has been enlisted in the "world ranking top 2% scientists" list (Stanford University, many years).